THE JOURNAL OF BIOLOGICAL CHEMISTRY VOL. 287, NO. 25, pp. 20876–20887, June 15, 2012


# Increased Resting Intracellular Calcium Modulates NF-κB-dependent Inducible Nitric-oxide Synthase Gene Expression in Dystrophic *mdx* Skeletal Myotubes*[S]

Received for publication, January 24, 2012, and in revised form, April 19, 2012 Published, JBC Papers in Press, May 1, 2012, DOI 10.1074/jbc.M112.344929

**Francisco Altamirano[‡], Jose R. López[§], Carlos Henríquez[‡], Tadeusz Molinski[¶], Paul D. Allen[§], and Enrique Jaimovich[‡1]**

*From the [‡]Centro de Estudios Moleculares de la Célula, Instituto de Ciencias Biomédicas, Facultad de Medicina, Universidad de Chile, Santiago 8389100, Chile, the [§]Department of Anesthesiology Perioperative and Pain Medicine, Brigham and Women's Hospital, Harvard Medical School, Boston, Massachusetts 02115, and the [¶]Department of Chemistry and Biochemistry and Skaggs School of Pharmacy and Pharmaceutical Sciences, University of California at San Diego, La Jolla, California 92093*

**Background:** The mechanisms by which NF-κB signaling is up-regulated in dystrophic muscles are unclear.
**Results:** $[Ca^{2+}]_{rest}$ is elevated in *mdx* myotubes as a result of both sarcolemmal $Ca^{2+}$ entry and SR release, resulting in NF-κB-induced iNOS expression.
**Conclusion:** $Ca^{2+}$ alterations at rest modulate NF-κB transcriptional activity and pro-inflammatory gene expression.
**Significance:** This allows for understanding the mechanism that relates elevated resting calcium and altered gene expression in muscular dystrophy.

**Duchenne muscular dystrophy (DMD) is a genetic disorder caused by dystrophin mutations, characterized by chronic inflammation and severe muscle wasting. Dystrophic muscles exhibit activated immune cell infiltrates, up-regulated inflammatory gene expression, and increased NF-κB activity, but the contribution of the skeletal muscle cell to this process has been unclear. The aim of this work was to study the pathways that contribute to the increased resting calcium ($[Ca^{2+}]_{rest}$) observed in *mdx* myotubes and its possible link with up-regulation of NF-κB and pro-inflammatory gene expression in dystrophic muscle cells. $[Ca^{2+}]_{rest}$ was higher in *mdx* than in WT myotubes (308 ± 6 *versus* 113 ± 2 nM, $p < 0.001$). In *mdx* myotubes, both the inhibition of $Ca^{2+}$ entry (low $Ca^{2+}$ solution, $Ca^{2+}$-free solution, and $Gd^{3+}$) and blockade of either ryanodine receptors or inositol 1,4,5-trisphosphate receptors reduced $[Ca^{2+}]_{rest}$. Basal activity of NF-κB was significantly up-regulated in *mdx versus* WT myotubes. There was an increased transcriptional activity and p65 nuclear localization, which could be reversed when $[Ca^{2+}]_{rest}$ was reduced. Levels of mRNA for TNFα, IL-1β, and IL-6 were similar in WT and *mdx* myotubes, whereas inducible nitric-oxide synthase (iNOS) expression was increased 5-fold. Reducing $[Ca^{2+}]_{rest}$ using different strategies reduced iNOS gene expression presumably as a result of decreased activation of NF-κB. We propose that NF-κB, modulated by increased $[Ca^{2+}]_{rest}$, is constitutively active in *mdx* myotubes, and this mechanism can account for iNOS overexpression and the increase in reactive nitrogen species that promote damage in dystrophic skeletal muscle cells.**

Duchenne muscular dystrophy (DMD)[2] is a lethal human X-linked genetic disorder caused by mutations in the *dystrophin* gene (1). DMD is a progressive muscle-wasting disease characterized by loss of the ability to walk between 6 and 12 years of age and death, caused by respiratory failure and cardiac dysfunction in their twenties (2). Like humans with DMD, *mdx* mice lack dystrophin due to an X-linked mutation providing an accepted model to study the human disease (1). In normal skeletal muscle, dystrophin is associated with a complex of glycoproteins known as dystrophin-glycoprotein complex, providing a linkage between the extracellular matrix and cytoskeleton (3). Dystrophin has an important role in stabilizing the sarcolemma, so in muscle fibers that lack this protein, membrane damage is recurrent (4, 5). However, although membrane fragility is an important factor, it does not fully explain the onset and progression of DMD.

The microenvironment of dystrophic muscle consists of activated immune cell infiltrates and up-regulated inflammatory gene expression (6). Nuclear factor-κB (NF-κB) consists of a family of transcription factors that play critical roles in inflammation, immunity, cell proliferation, differentiation, and survival (7). The NF-κB transcription factor family in mammals consists of five proteins, p65 (RelA), RelB, c-Rel, p105/p50 (NF-κB1), and p100/52 (NF-κB2), that form homo- and heterodi-

* This work was supported, in whole or in part, by National Institutes of Health Grants AR43140 and AR052354 (to P. D. A. and J. R. L.). This work was also supported by Grants Fondo Nacional de Investigación Cientifica y Tecnológica 1110467, Fondo de Financiamiento de Centros de Excelencia en Investigación 15010006, and Asotiation Francaise Contre les Myopathies 14562 (to E. J.), Grant AT-24100066 from Comisión Nacional de Investigación Cientifica y Tecnológica, Vicerrectoría de Asuntos Académicos, Universidad de Chile, and Programa de Mejoramiento de lo Calidad y Equidad de la Educación travel support UCH 0714, Universidad de Chile (to F. A.).
[S] This article contains supplemental Figs. S1–S3.
[1] To whom correspondence should be addressed: Instituto de Ciencias Biomédicas, Facultad de Medicina, Universidad de Chile, Casilla 70005, Santiago 7, Chile. E-mail: ejaimovi@med.uchile.cl.

[2] The abbreviations used are: DMD, Duchenne muscular dystrophy; iNOS, inducible nitric-oxide synthase; $IP_3$, inositol 1,4,5-trisphosphate receptor; Ry, ryanodine; RyR, ryanodine receptor; SR, sarcoplasmic reticulum; XeC, xestospongin C; SOCE, store-operated calcium entry; B5, bastadin 5; IKK, IκBα kinase; DAF-FM diacetate, 4-amino-5-methylamino-2′,7′-difluorofluorescein diacetate.

meric complex (7). NF-κB has been implicated in *mdx* pathology, because blockade of this pathway through pharmacological or genetic approaches improves muscle histology, reduces pro-inflammatory gene expression, and ameliorates damage (8–12). NF-κB activity is increased in muscles from *mdx* mice and DMD patients (10, 13–15). The p65/p50 heterodimer is the predominant form of NF-κB in most cells and controls the expression of a wide array of genes critical in the immune response and inflammation (16). IkBα retains the p65/p50 heterodimer in the cytoplasm. Upon stimulation, IkBα is quickly phosphorylated by the IKK complex, ubiquinated, and degraded, thus allowing the translocation to the nucleus of the NF-κB complex (7).

IKKα/β or p65 gene ablation in transgenic animals or by adeno-associated virus improves pathology in *mdx* mouse muscles (8–12). Acharyya *et al.* (10) have shown that NF-κB activity can be seen in both muscle and immune cells and that *mdx* muscle pathology was improved in *mdx*/p65$^{+/-}$ but not *mdx*/p50$^{+/-}$ mice.

NF-κB gene targets, such as the pro-inflammatory cytokines TNF-α, IL-1β, IL-6, and iNOS are up-regulated in muscles from Duchenne patients and *mdx* mice (10, 17–20). In *mdx* mice, injections of the nonspecific NF-κB inhibitor curcumin have been shown to reduce NF-κB activation and TNF-α, IL-1β, and iNOS expression (6, 9).

iNOS or NOS2, originally discovered in cytokine-induced macrophages, is a largely calcium-independent NOS, which is expressed at highest levels in immunologically activated cells and is normally absent in resting cells (21). iNOS expression is increased in muscles from *mdx* mice and can be reversed by curcumin (9, 22, 23). High levels of nitric oxide (NO) production lead to the formation of peroxynitrite, a highly reactive species contributing to muscle oxidative damage (21, 24). In addition, iNOS expression has been associated with *S*-nitrosylation of type 1 ryanodine receptor (RyR1), calcium dysregulation, and muscle pathology in *mdx* mice (22).

Although there are many examples in the literature indicating that resting intracellular free $Ca^{2+}$ concentration ($[Ca^{2+}]_{rest}$) is higher in skeletal muscle cells from *mdx* mice and DMD patients compared with normal cells (25–30), others authors have not (31, 32). The mechanism that has been proposed for causing this elevation in $[Ca^{2+}]_{rest}$ assumes recurrent membrane damage due the failure of dystrophin function to stabilize the sarcolemma (5, 33), allowing $Ca^{2+}$ leak into the cell through the damaged membrane. An alternative explanation is an increased $Ca^{2+}$ entry through transient receptor potential channel 1 (TRPC1) and hyperactive store-operated calcium entry (SOCE) in *mdx* muscle fibers (25, 34–38).

Several studies have shown that NF-κB activity can be modulated by intracellular $Ca^{2+}$ levels (39–42). In skeletal muscle cells, depolarization with high $K^+$ or electrical stimulation activates NF-κB through $Ca^{2+}$ signals elicited by the ryanodine (RyR) and inositol 1,4,5-triphosphate ($IP_3R$) receptors (40).

In dystrophic muscle cells, increased $[Ca^{2+}]_{rest}$, has been mainly thought to cause necrosis through calpain activation and mitochondrial permeability transition pore (29, 43, 44). Here, we have revisited the issue of elevated $[Ca^{2+}]_{rest}$ in dystrophic *mdx* skeletal muscle cells showing that it is a complex process that involves sarcolemmal $Ca^{2+}$ entry as well as SR $Ca^{2+}$ leak, both through RyRs and $IP_3Rs$. In addition, we demonstrate that the level of $[Ca^{2+}]_{rest}$ modulates the transcription factor NF-κB activity and iNOS expression in *mdx* myotubes.

## MATERIALS AND METHODS

*Cell Culture*—All procedures for animal use were in accordance with guidelines approved by the Bioethical Committee at the Facultad de Medicina, Universidad de Chile. Primary myotubes from wild type C57BL/6 and *mdx* mice were isolated according to the method of Rando and Blau (45). The myoblasts were grown and differentiated as described previously (46).

*Determination of $[Ca^{2+}]_{rest}$ by $Ca^{2+}$-selective Microelectrodes*—Double-barreled $Ca^{2+}$-selective microelectrodes were prepared and calibrated as described previously (47). Only those electrodes with a linear relationship between *p*Ca3 and *p*Ca8 (Nernstian response, 28.5 mV per *p*Ca unit at 24 °C) were used experimentally. To better mimic the intracellular ionic conditions, all calibration solutions were supplemented with 1 mM $Mg^{2+}$. All electrodes were then re-calibrated after making measurements of $[Ca^{2+}]_{rest}$, and if the two calibration curves did not agree within 3 mV from *p*Ca7 to *p*Ca8, the data from that microelectrode was discarded. Myotubes were impaled with the double-barreled microelectrode, and potentials were recorded via high impedance amplifier (WPI Duo-773). The potential from the 3 M KCl barrel ($V_m$) was subtracted electronically from $VCa_E$ to produce a differential $Ca^{2+}$-specific potential ($V_{Ca}$) that represents the $[Ca^{2+}]_{rest}$. $V_m$ and $V_{Ca}$ were filtered (30–50 KHz) to improve the signal-to-noise ratio and stored in a computer for further analysis. The experiments were performed in Krebs-Ringer solution (in mM: 125 NaCl, 5 KCl, 2 $CaCl_2$, 1.2 $MgSO_4$, 6 glucose, and 25 Hepes/Tris, pH 7.4). The low $Ca^{2+}$ solution was prepared replacing the $CaCl_2$ with $MgCl_2$ (≈7 μM $Ca^{2+}$). $Ca^{2+}$-free solution was prepared by omitting $Ca^{2+}$ and adding $Mg^{2+}$ (2 mM) and EGTA (2 mM). We avoided measurements of $[Ca^{2+}]_{rest}$ after long incubations in both solutions (more than 5 min) because, despite the fact that the solution was supplemented with 2 mM $Mg^{2+}$, all myotubes began to show a significant depolarization (>8 mV) after this interval.

In every experiment, we determined the $[Ca^{2+}]_{rest}$ in control conditions in both WT and *mdx* myotubes, and data were expressed as the total average for basal $[Ca^{2+}]_{rest}$ for WT and *mdx* myotubes (Fig. 1).

*Sarcoplasmic Reticulum $Ca^{2+}$ Content*—To estimate the total amount of $Ca^{2+}$ stored in the intracellular compartments, primarily from the SR stores, myotubes were loaded with 5 μM Fluo-4-AM or Fluo-5N-AM for 30 min at 37 °C. Cells were placed on the stage of an inverted microscope equipped with epifluorescence illumination (XCite® Series 120 or Lambda DG4) equipped with a CCD cooled camera (Retiga 2000R or Stanford Photonics 12 bit digital). The cell-containing coverslips or μ-clear 96-well/plates (Greiner Bio-one) were placed in the microscope for fluorescence measurements after excitation with a 488-nm wavelength filter system (Lambda 10–2 or DG4, Sutter Instruments). The emission signal was acquired at a frequency of 10 frames/s. The amount of SR $Ca^{2+}$ was estimated by taking the area under the curve of the signal induced by 5 μM

ionomycin in $Ca^{2+}$-free solution to minimize $Ca^{2+}$ entry. Fluorescence data (F) was analyzed by normalizing with respect to basal fluorescence ($F_0$) and expressed as $(F - F_0)/F_0$.

*Resting $Ca^{2+}$ Entry*—Myotubes were loaded with Fura2-AM (5 μM) for 30 min at 37 °C and the cells were perfused with low $Ca^{2+}$ solution for 1 min; then the perfusion system was switched to $Mn^{2+}$-containing solution (in mM: 125 NaCl, 5 KCl, 0.5 $MnCl_2$, 2.7 $MgSO_4$, 6 glucose, and 25 Hepes/Tris, pH 7.4) for 1 min. During the quench, the perfusion system was switched to $Mn^{2+}$ containing solution with gadolinium trichloride for an additional 1 min ($Gd^{3+}$, 20 μM), to study the effect of the later on $Ca^{2+}$ entry. To calculate the fluorescence quench rate, the stable part of the signal was fitted to a linear regression. The derived slope was expressed as fluorescence arbitrary units/s. The excitation wavelength used to measure $Mn^{2+}$ quench of Fura-2 was monitored using a 357/7-nm excitation and 510/80-nm emission filter.

*Immunofluorescence and Confocal Microscopy*—For immunofluorescence localization of the NF-κB p65 subunit, differentiated myotubes were fixed in 4% paraformaldehyde for 10 min at RT. Cells were rinsed with PBS, then blocked with PBS, 1% BSA for 1 h at room temperature, and incubated overnight with p65 antibody at a 1:200 dilution at 4 °C. Cells were washed and then incubated for 1 h with Alexa Fluor-488 anti-rabbit antibody (Invitrogen). Hoechst was used for nuclear visualization. Immunofluorescence was observed in a confocal microscope (Carl Zeiss, Axiovert 200, LSM 5-Pascal) and images were deconvolved using Iterative Deconvolution software of ImageJ. To determine the nuclear localization of the NF-κB p65 subunit, the fluorescence intensity of nuclear and cytosolic region of interest was calculated for at least 10 different myotubes in three different experiments and averaged to calculate the ratio of nuclear over cytoplasmic intensity using the ImageJ program. *z*-stack images were reconstructed using the Interactive 3D Surface Plot ImageJ plugin (rsb.info.nih.gov) that translates the luminance of an image as height for the plot. DAF-FM diacetate (Molecular Probes) fluorescence was detected according to the manufacturer's instructions by confocal microscopy with an excitation 488 nm wavelength argon laser.

*Western Blot*—Total protein lysates were prepared from differentiated myotubes by homogenizing them in a lysis buffer containing 20 mM Tris-HCl, pH 7.5, 1% Triton X-100, 1 mM EDTA, 1 mM EGTA, 20 mM NaF, 1 mM $Na_2P_2O_7$, 10% glycerol, 150 mM NaCl, 10 mM $Na_3VO_4$, 1 mM PMSF, and protease inhibitors (Complete™, Roche Applied Science). Proteins were separated using SDS-PAGE and transferred to PVDF membranes. The following primary antibodies and their dilutions were used: NF-κB p65 subunit (1:1000; Cell Signaling); iNOS (1:2000; Santa Cruz Biotechnology); GAPDH (1:2000, Santa Cruz Biotechnology); and β-actin (1:10,000, Sigma). The protein bands in the blots were visualized using an ECL detection kit (Pierce), and the intensity of the bands was determined with ImageJ densitometric analysis.

*siRNA Transfection*—NF-κB p65 and scramble siRNA were purchased from Santa Cruz Biotechnology. NF-κB p65 siRNA is a pool of four target-specific double-stranded siRNAs. Myoblasts at 50–70% confluence were transfected with both siRNAs (50 nM) with DharmaFECT Duo (Dharmacon) for 3 h at 37 °C and 5% $CO_2$ in 35-mm culture plates in Opti-MEM (Invitrogen). Following transfection, myoblasts were differentiated for 48 h and lysed for protein detection by Western blot.

*NF-κB Luciferase Reporter Activity Determinations*—A plasmid containing five tandems repeats of NF-κB-binding sites cloned upstream of a luciferase reporter gene (pNF-κB-Luc) was obtained from Agilent Technologies and subcloned in a lentiviral vector with neomycin resistance, and lentiviral particles were produced by transient transfection of HEK 293T cells as described (48). Supernatants were collected, and myoblast cultures were transduced immediately after isolation at a multiplicity of infection of 1:500 in the presence of 6 μg/ml protamine sulfate for 3 h. Cells were allowed to recover for 48 h and then selected with neomycin (400 μg/ml) for 9 days. After infection and selection, myoblasts were completely normal and differentiated into myotubes similarly to uninfected cells. To minimize clonal variations, we pooled together more than 100 G418-resistant clones from each transduction to perform the experiments. Luciferase activity was determined using a Dual-Luciferase reporter assay system (Promega) according to the manufacturer's instructions, and light detection was carried out in a Berthold F12 luminometer. Results were normalized with total protein, and the relation "luciferase $mg^{-1}$ protein" was shown. We studied the response to lipopolysaccharide (LPS), a strong activator of NF-κB as a control (data not shown).

*Real Time PCR*—Total RNA from myotubes cultures was obtained using TRIzol reagent (Invitrogen) according to the manufacturer's protocol. cDNA was prepared by reverse transcription of 1 μg of total RNA, using SuperScript II (Invitrogen). Real time PCR was performed using a Stratagene Mx3000P as follows. Primers were used at a final concentration of 400 nM. Briefly, 1–4 μl of cDNA reaction together with the appropriate primers was added to 10 μl of Brilliant III UltraFast SYBR Green QPCR master mix (Agilent Technologies) to a total volume of 20 μl. No-template control reactions were also prepared for each gene. The cycling parameters for all genes were as follows: 95 °C for 3 min, then 50 cycles of 95 °C for 20 s, and 60 °C for 20 s. Expression values were normalized to GAPDH and are reported in units of $2^{-\Delta\Delta Ct} \pm$ S.E (49). PCR products were verified by melting-curve analysis, resolved by electrophoresis on 2% agarose gel, and stained with ethidium bromide.

The TNF-α, IL-1β, IL-6, iNOS, and GAPDH mRNA transcripts were quantified using oligonucleotide primers designed based on sequences published in NCBI GenBank™ with the open-source PerlPrimer software (50). The forward and reverse primers sequences used in this study are shown in Table 1.

*Statistics*—All values are expressed as mean ± S.E. from at least three different determinations. Results of luciferase activity, p65 immunofluorescence, DAF-FM fluorescence, and Western blot were transformed with the WT basal average ($y = y'/(\text{WT basal average})$) to normalize to 1 with S.E. Statistical analysis was performed using an unpaired two-tailed *t* test or analysis of variance-Bonferroni to determine significance ($p < 0.05$).

## RESULTS

*$[Ca^{2+}]_{rest}$ Is Increased in Dystrophic mdx Myotubes*—Resting membrane potentials ($V_m$) and $[Ca^{2+}]_{rest}$ were measured in dif-

**TABLE 1**
**Oligonucleotides used for detection of mRNA levels by real time PCR in myotubes derived from WT and *mdx* mice primary culture**

| mRNA | Accession no. | Forward primer (5′ → 3′) | Reverse primer (5′ →3 ′) | Amplicon | Source or Ref. |
|---|---|---|---|---|---|
| | | | | *bp* | |
| GAPDH | NM_008084.2 | CTCATGACCACAGTCCATGC | TTCAGCTCTGGGATGACCTT | 155 | This study |
| iNOS | NM_010927.3 | CAGCTCAAGAGCCAGAAACG | TTACTCAGTGCCAGAAGCTG | 141 | This study |
| IL-1β | NM_008361.3 | CTTTGAAGAAGAGCCCATCC | TTTGTCGTTGCTTGGTTCTC | 229 | This study |
| IL-6 | NM_031168.1 | CCAATTTCCAATGCTCTCCT | ACCACAGTGAGGAATGTCCA | 182 | (83) |
| TNF-α | NM_013693.2 | TCACACTCAGATCATCTTCTC | ATGAGATAGCAAATCGGCTG | 261 | This study |

ferentiated WT and *mdx* myotubes with $Ca^{2+}$-selective microelectrodes. The $[Ca^{2+}]_{rest}$ observed in *mdx* myotubes was significantly higher than that observed in WT myotubes (308 ± 6 nM, $n = 38$ *versus* 113 ± 2 nM, $n = 20$, $p < 0.001$) (Fig. 1*A*). $V_m$ was significantly increased in *mdx* myotubes compared with the WT counterpart (−50 ± 0.2 mV, $n = 38$ *versus* −62 ± 0.2 mV, $n = 20$, $p < 0.001$) (Fig. 1*B*).

*Blockade of $Ca^{2+}$ Entry in mdx Myotubes Reduced but Did Not Normalize $[Ca^{2+}]_{rest}$*—Several studies have suggested that $[Ca^{2+}]_{rest}$ is increased in *mdx* skeletal muscle cells, due to an increased $Ca^{2+}$ entry from extracellular space through TRPC1 and/or SOCE channels (25, 34–38). To explore the contribution of extracellular $Ca^{2+}$ to $[Ca^{2+}]_{rest}$ in WT and *mdx* myotubes, we used four different strategies as follows: low $Ca^{2+}$ solution, $Ca^{2+}$-free solution, Krebs-Ringer solution supplemented with gadolinium trichloride ($Gd^{3+}$, 20 μM), and $Ca^{2+}$-free solution with $Gd^{3+}$(see under "Materials and Methods"). Cells were incubated for 2 min before $[Ca^{2+}]_{rest}$ determinations were made. We observed a nonsignificant reduction in $[Ca^{2+}]_{rest}$ in WT myotubes after the addition of low $Ca^{2+}$ solution, $Ca^{2+}$-free solution, and $Gd^{3+}$ solution (92.9 ± 1 nM, $n =$ 20, 91.0 ± 1 nM, $n = 15$, and 86.3 ± 1 nM, $n = 20$, all $p > 0.05$ compared with the WT basal value) (Fig. 2*A*). In *mdx* myotubes, there was a significant decrease in $[Ca^{2+}]_{rest}$ in all conditions (184 ± 8 nM, $n = 12$, with low $Ca^{2+}$, 148 ± 6 nM in $Ca^{2+}$ free solution, $n = 10$, 147 ± 1 nM, $n = 11$, after $Gd^{3+}$, all of them $p <$ 0.001 compared with the *mdx* basal value) (Fig. 2*A*). The addition of $Gd^{3+}$ to the $Ca^{2+}$-free solution did not cause a further reduction of $[Ca^{2+}]_{rest}$, suggesting that $Gd^{3+}$ by itself was able to block the active $Ca^{2+}$-entry pathway. In addition, we estimated $Ca^{2+}$ entry by $Mn^{2+}$ quench of Fura-2 fluorescence. Rates of $Mn^{2+}$ quench were significantly higher in *mdx* myotubes (Fig. 2, *B* and *C*), and this was completely blocked by the addition of $Gd^{3+}$ (20 μM). Although inhibition of $Ca^{2+}$ entry by either $Gd^{3+}$ or removal of extracellular $Ca^{2+}$ reduced $[Ca^{2+}]_{rest}$ in *mdx* myotubes, it did not return it to WT levels, suggesting an additional mechanism(s) causing $[Ca^{2+}]_{rest}$ dysregulation in *mdx* myotubes.

*Inhibition of RyRs and $IP_3Rs$ Reduced $[Ca^{2+}]_{rest}$ in mdx Myotubes*—We have previously reported that $[Ca^{2+}]_{rest}$ depends largely on a Ry-insensitive leak by RyR1 ("RyR1 leak") and was unaffected by Ry treatment (47). Bastadin 5 (B5), a brominated macrocyclic derivative of dityrosine, isolated from the marine sponge *Icanthellabasta* (51), interacts with RyR1, modulating RyR1 gating behavior in an FKBP12-dependent manner. B5 can be used as a pharmacological tool to convert RyR1 from its leak conformation into a gating conformation, restoring the Ry sensitivity (47). We studied the contribution of RyR1 to the $[Ca^{2+}]_{rest}$ in *mdx* myotubes (Fig. 3*A*). Ry treatment

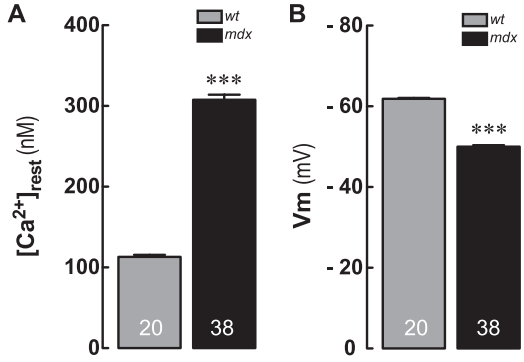


FIGURE 1. *A,* resting intracellular $Ca^{2+}$ concentrations ($[Ca^{2+}]_{rest}$); *B,* resting membrane potentials ($V_m$) measured by double-barreled microelectrodes in WT and *mdx* primary myotubes. Data are expressed as means ± S.E., $n = 20$ for WT and $n = 38$ for *mdx*, indicated inside the *bars*. ***, $p < 0.001$ *versus* WT.

alone did not modify $[Ca^{2+}]_{rest}$ in WT myotubes but did cause a significant reduction of $[Ca^{2+}]_{rest}$ in *mdx* myotubes (99 ± 3 nM, $n = 15$, $p > 0.05$, 213 ± 5 nM, $n = 19$, $p < 0.001$ compared with WT and *mdx* basal values, respectively). Addition of B5 in the presence of Ry significantly diminished $[Ca^{2+}]_{rest}$ in both WT and *mdx* myotubes (80 ± 1 nM, $n = 9$, $p < 0.05$, 166 ± 9 nM, $n = 9$, $p < 0.001$ compared with WT and *mdx* basal values, respectively) but also did not reduce *mdx* basal values to those seen in WT.

We have previously demonstrated that the expression of $IP_3Rs$, as well as the total mass of inositol 1,4,5-trisphosphate, is increased in both *mdx* and human DMD-derived cell lines compared with normal cells (52). U-73122 (a PLC inhibitor) and Xestospongin C (an $IP_3R$ blocker) significantly reduced the $[Ca^{2+}]_{rest}$ only in *mdx* myotubes (241 ± 7 nM, $n = 24$, and 232 ± 6 nM, $n = 20$, respectively, both $p < 0.001$ compared with the *mdx* basal value), without any significant effect in WT myotubes (113 ± 2 nM, $n = 21$, and 97 ± 2 nM, $n = 16$, respectively, $p > 0.05$ compared with WT basal values) (Fig. 3*A*), whereas U-73343 (an inactive PLC inhibitor) did not modify $[Ca^{2+}]_{rest}$ in either WT or *mdx* myotubes.

To quantify the level of the SR $Ca^{2+}$ store, we exposed WT and *mdx* myotubes loaded with Fluo-4-AM to 5 μM ionomycin in $Ca^{2+}$-free solution. Under these conditions, the total $Ca^{2+}$ released was significantly smaller in *mdx* myotubes compared with WT myotubes (area under curve = 23.7 ± 2.4 *versus* 40.4 ± 4.2, $p < 0.01$) (Fig. 3, *B* and *C*, and representative fluorescence images in supplemental Fig. S1). Similar results were obtained in Fluo-5N-loaded myotubes (supplemental Fig. S2). Moreover, treatment (3 h) with either Ry (30 μM) or XeC (5 μM), partially restored the SR $Ca^{2+}$ content in *mdx* myotubes (Fig. 3*C*), suggesting that the reduction in the SR $Ca^{2+}$ levels is

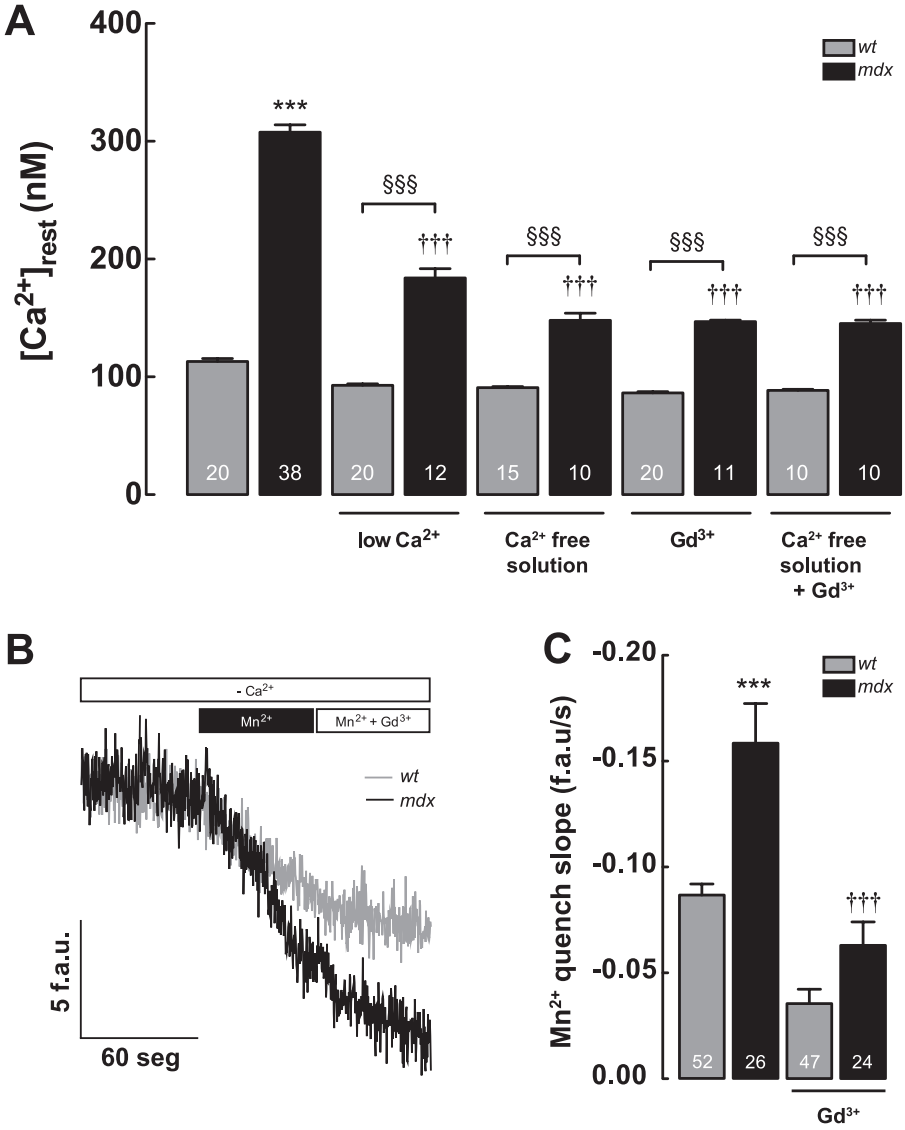


FIGURE 2. **$Ca^{2+}$ entry contribution to $[Ca^{2+}]_{rest}$ measured in WT and *mdx* myotubes.** *A,* effects of removal of extracellular $Ca^{2+}$ (low $Ca^{2+}$ solution and $Ca^{2+}$-free solution) and $Gd^{3+}$ treatment on $[Ca^{2+}]_{rest}$. *B* and *C,* measurements of resting $Ca^{2+}$ entry using $Mn^{2+}$ quench in WT and *mdx* myotubes. *B,* representative traces of Fura-2 fluorescence quench by $Mn^{2+}$ measured under resting conditions. *C,* quantification of the rate of $Mn^{2+}$ quench, between WT and *mdx* myotubes. $Gd^{3+}$ (20 $\mu$M) was added during the experimental determination of $Mn^{2+}$ quench as shown in figure. Data are expressed as mean ± S.E. ***, $p <$ 0.001 *versus* WT basal value; †††, $p < 0.001$ *versus mdx* basal value. §§§, $p < 0.001$ is indicated in the figure. *f.a.u./s,* fluorescence arbitrary units/s.

due to a $Ca^{2+}$ leak from the SR through both RyRs and $IP_3Rs$ that modulates $[Ca^{2+}]_{rest}$.

*NF-κB Activity Is Up-regulated in Dystrophic Myotubes and Can Be Reversed with Inhibitors That Reduce $[Ca^{2+}]_{rest}$*—We studied the subcellular distribution of the p65 subunit of NF-κB. Fig. 4*A* shows an increased nuclear localization of p65 in *mdx* myotubes compared with WT myotubes, measured by immunofluorescence and confocal microscopy. Three-dimensional reconstruction of *z*-stack images shows that p65 is located primarily in the cytosol, but in *mdx* myotubes, the distribution is diffuse with both cytoplasmic and nuclear localization. Basal fluorescence ratio of p65 between nucleus and cytosol was increased about 50% in dystrophic myotubes compared with normal myotubes (Fig. 4*B*). We assessed the transcriptional activity of NF-κB using a reporter that contains five tandems repeats of NF-κB-binding sites cloned upstream of a luciferase gene (see "Materials and Methods"). Luciferase activity was increased 2.5-fold in *mdx* myotubes compared with WT myotubes (Fig. 4*C*). To establish a correlation between $[Ca^{2+}]_{rest}$ and NF-κB transcriptional activity, we treated myotubes for 6 h with $Gd^{3+}$, Ry, and XeB (53, 54) as described previously at the same concentrations. None of these drugs caused a significant change in the luciferase reporter activity in WT myotubes ($p > 0.05$) (Fig. 4*C*). However, blockade of sarcolemmal $Ca^{2+}$ entry with $Gd^{3+}$ reduced the luciferase reporter activity by 19% ($p > 0.05$), and pretreatment with Ry or XeB reduced it by 58 and 38%, in *mdx* myotubes, respectively ($p < 0.001$ and $p < 0.01$, respectively, compared with the *mdx* basal value). Furthermore, 1,2-bis(2-aminophenoxy)ethane-*N*,*N*,*N*′,*N*′-tetraacetic acid tetrakis(acetoxymethyl ester) (BAPTA AM, 50 $\mu$M) treatment reduced NF-κB transcriptional activity in *mdx* myotubes by 43% ($p < 0.05$) without any significant effect in WT myotubes. To confirm the contribution of $Ca^{2+}$ released by SR, we measured the subcellular distribution

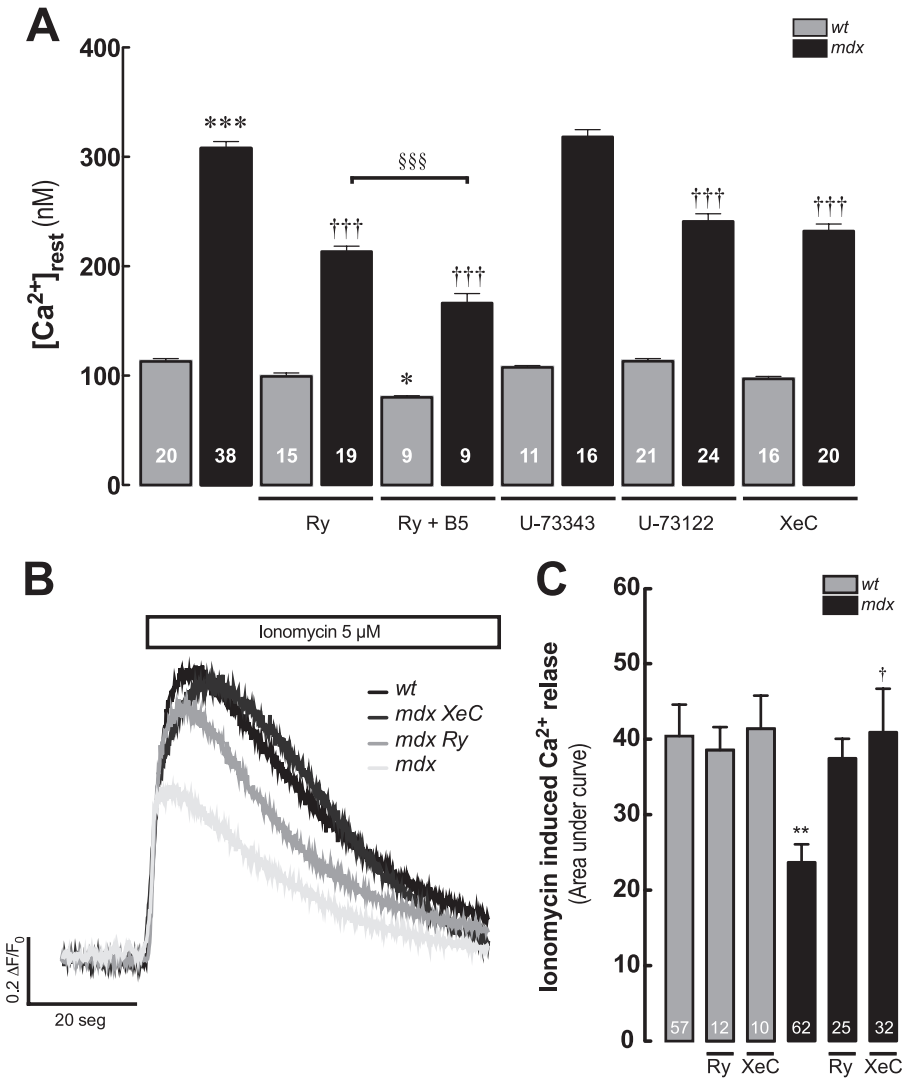


FIGURE 3. **RyR and $IP_3R$ participation in $[Ca^{2+}]_{rest}$ in WT and *mdx* myotubes.** *A,* effect of Ry (30 μM), Ry + B5 (Ry, 30 μM, and B5, 10 μM), U-73343 (5 μM), U-73122 (5 μM), and XeC (5 μM) on $[Ca^{2+}]_{rest}$ (treatments for 3 h). *B,* representative traces of Fluo-4 fluorescence signals after the addition of 5 μM ionomycin, in the absence of extracellular $Ca^{2+}$ ($Ca^{2+}$-free solution) in WT, *mdx,* and Ry- and XeC-treated *mdx* myotubes. *C,* average area under the curve of the ionomycin-induced $Ca^{2+}$ transients. Data are expressed as means ± S.E. ***, $p < 0.001$; **, $p < 0.01$; *, $p < 0.05$ *versus* WT basal value, †, $p < 0.05$; †††, $p < 0.001$ *versus mdx* basal value. §§§, $p < 0.001$ is indicated in the figure.

of p65 in the presence of Ry or XeB. Both inhibitors reduced nuclear/cytosol p65 fluorescence by *mdx* myotubes (Fig. 4*B*).

*TNF-α, IL-1β, and IL-6 Gene Expression Was Similar in WT and mdx Myotubes*—To identify gene targets that can be modulated by $[Ca^{2+}]_{rest}$-dependent NF-κB up-regulation, we studied the levels of mRNA for TNF-α, IL-1β, and IL-6 in both myotube models. We did not observe any significant difference in the mRNA levels of these cytokines between WT and *mdx* myotubes under resting conditions (supplemental Fig. S3).

*iNOS Is Overexpressed in mdx Myotubes and Is Dependent on $[Ca^{2+}]_{rest}$ and NF-κB Activity*—We observed increased iNOS mRNA levels and protein expression in *mdx* myotubes ($p < 0.001$ and $p < 0.01$, respectively, compared with WT myotubes) (Fig. 5, *A* and *B*). Moreover, nitric oxide (NO) production, assessed by DAF-FM fluorescence, was ≈20% higher in *mdx* compared with WT myotubes (Fig. 5*C*). In myotubes transfected with p65 siRNA, the expression of p65 protein, after 48 h, was reduced by 89 and 82% in WT and *mdx* myotubes, respectively (Fig. 5*D*). p65 knockdown in *mdx* myotubes normalized iNOS protein levels to WT values showing that the latter is regulated by the activity level of the former (Fig. 5*D*). Moreover, treatment with compounds that lower $[Ca^{2+}]_{rest}$ for 6 h significantly reduced iNOS mRNA levels in *mdx* myotubes (75% $Gd^{3+}$, 86% Ry, and 66% XeB), but it had no significant effect in WT myotubes (Fig. 5*A*).

*p38 MAPK Is Involved in NF-κB Up-regulation in mdx Myotubes*—Several $Ca^{2+}$-sensitive pathways can modulate the activity of the NF-κB signaling pathway (41, 55). To determine the signal transduction pathways involved in the $[Ca^{2+}]_{rest}$-dependent NF-κB up-regulation, we used specific pharmacological blockers for ERK1/2, JNK, p38 MAPKs, $Ca^{2+}$/calmodulin-dependent kinase II, calcineurin A, and protein kinase C (PKC) (Fig. 6). Only p38 MAPK inhibition with SB-203580 (10 μM) significantly reduced the NF-κB luciferase reporter activity in both WT and *mdx* myotubes by 82 and 73%, respectively ($p < 0.001$).

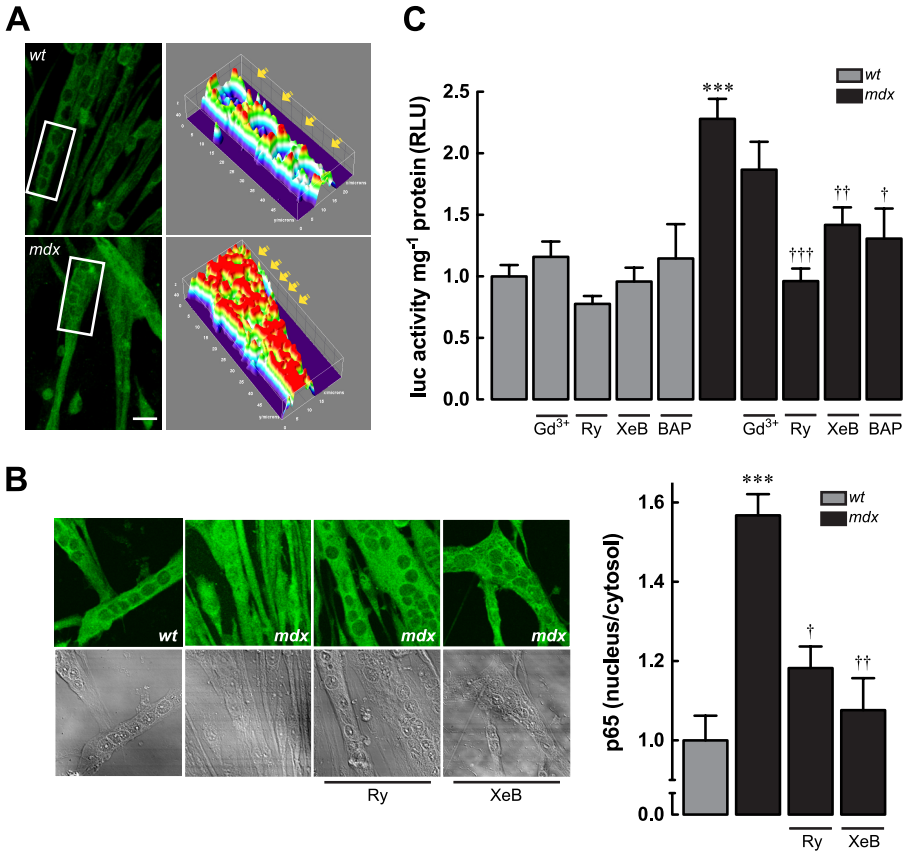


FIGURE 4. **NF-κB activity in WT and *mdx* myotubes.** *A, left panel*, representative *z*-stack immunofluorescence images obtained by confocal microscopy; *right panel*, three-dimensional reconstructions made with the ImageJ (National Institutes of Health) plugin Interactive 3D Surface Plot. *B,* effect of SR $Ca^{2+}$ release inhibition in p65 subcellular distribution. *C,* NF-κB luciferase reporter activity in WT and *mdx* myotubes treated with $Ca^{2+}$ inhibitors. Myotubes were incubated for 6 h and then lysed for luciferase activity determination. Data are expressed as mean ± S.E. from at least three different determinations, ***, $p < 0.001$ *versus* WT basal value, †††, $p < 0.001$; ††, $p < 0.01$ and †, $p < 0.05$ *versus mdx* basal value.

## DISCUSSION

In dystrophic skeletal muscle cells, increased $[Ca^{2+}]_{rest}$ has been mainly related with calpain activation and mitochondrial permeability transition pore aperture as factors that induce death in skeletal muscle fibers. Here, we show the first evidence that elevated $[Ca^{2+}]_{rest}$ in dystrophic myotubes causes altered function of the transcription factor NF-κB leading to iNOS expression. In addition, our data show that the increased $[Ca^{2+}]_{rest}$ in *mdx* myotubes is multifactorial, involving both $Ca^{2+}$ entry and $Ca^{2+}$ SR leak, through RyRs and $IP_3$Rs.

We have previously shown that the $[Ca^{2+}]_{rest}$ in DMD muscle fibers was ~370 nM, although in normal muscle fibers it was ~100 nM (27). Other authors have shown similar calcium concentrations in adult *mdx* fibers compared with the WT fibers (25, 28). A possible explanation to why some authors did not find elevated $[Ca^{2+}]_{rest}$ in dystrophic muscle cells may be due, in part, to methodological differences in fluorescent dye calibration, the previous contractile activity, and age of the fibers. Moreover, fluorescent dyes, as 1,2-bis(2-aminophenoxy)-ethane-*N*,*N*,*N*′,*N*′-tetraacetic acid derivatives, are $Ca^{2+}$ chelators and can artificially reduce $[Ca^{2+}]_{rest}$. Thus in most cases, the $[Ca^{2+}]_{rest}$ values that have been reported in muscle cells using this method are significantly lower (range 20–80 nM) than those reported using $Ca^{2+}$-selective microelectrodes (100–120 nM).

TRPC1-dependent $Ca^{2+}$ entry is increased in *mdx* muscle fibers (25, 34, 36). Both GsMTx4 and streptomycin reduced $[Ca^{2+}]_{rest}$ and prevented the rise of the $[Ca^{2+}]_{rest}$ following eccentric contractions improving the muscle function and increasing myofiber regeneration in *mdx* mice (25, 28, 36). In addition to stretch channel activation, SOCE has emerged as another contributor in increased resting $Ca^{2+}$ entry in *mdx* fibers (35, 37, 38). We have found that $Gd^{3+}$, an unspecific blocker of $Ca^{2+}$-entry through SOCE and transient receptor potential channels (56), reduced $[Ca^{2+}]_{rest}$ by 52% in *mdx* myotubes and that long term treatment with $Gd^{3+}$ was associated with a reduction in NF-κB activity and iNOS expression. However, blocking $Ca^{2+}$ entry did not completely normalize $[Ca^{2+}]_{rest}$, suggesting a possible intracellular contribution.

In primary *mdx* myotubes, treatment with Ry reduced the $[Ca^{2+}]_{rest}$ by 31% and adding B5 decreased it further to 46%. We have previously shown that $[Ca^{2+}]_{rest}$ depends largely on Ry-insensitive leak of RyR1 channels (RyR1 leak) that can be blocked by Ry + B5 treatment in normal myotubes (47). Bellinger *et al.* (22) have shown that RyR1 isolated from *mdx* skeletal muscle shows an age-dependent increase in *S*-nitrosylation coincident with muscle pathology, which depleted the channel complex of FKBP12, resulting in "leaky channels." Depletion of FKBP12 from RyR1 channel to nitrosative stress may render it sensitive to $Ca^{2+}$-mediated activation (22).

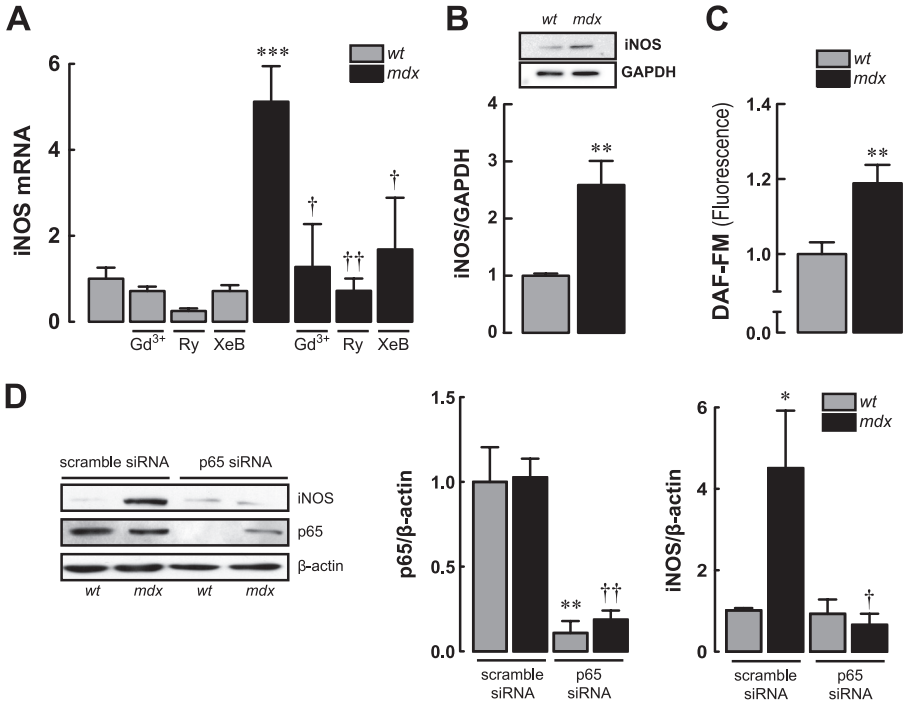


FIGURE 5. **iNOS expression in WT and *mdx* myotubes.** *A,* iNOS mRNA levels assessed by real time PCR showing effects of $[Ca^{2+}]_{rest}$ reduction on iNOS mRNA expression. *B,* iNOS protein expression determined by Western blot. *C,* levels of nitric oxide (*NO*) was determined with DAF-FM fluorescence probe with confocal microscopy. *D,* effects of p65 knockdown by siRNA in the levels of p65 and iNOS proteins expression determined by Western blot. Myoblasts were transfected and then differentiated to myotubes for 48 h before the protein determination. Data are expressed as means ± S.E. from at least three different determinations. ***, $p < 0.001$; **, $p < 0.01$ and *, $p < 0.05$ *versus* WT basal value, ††, $p < 0.01$ and †, $p < 0.05$ *versus mdx* basal value.

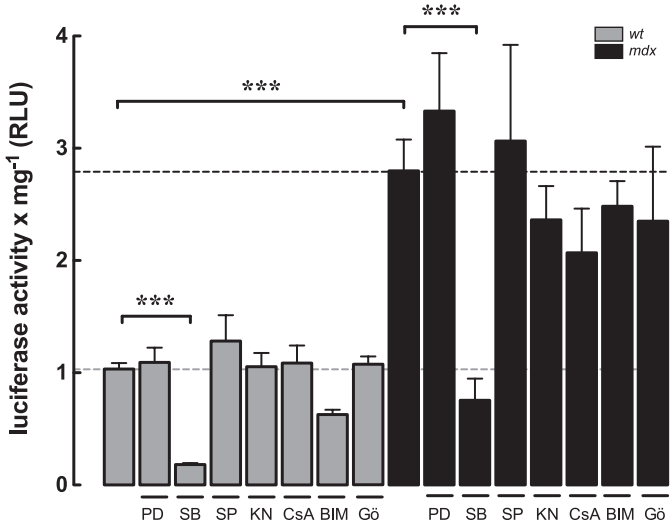


FIGURE 6. **NF-κB transcriptional activity is modulated by p38 MAPK activity in both WT and *mdx* myotubes.** Myotubes were treated with PD-98059 (*PD*) (ERK1/2 inhibitor, 10 μM), SB-203580 (*SB*) (p38 inhibitor, 10 μM), SP-600125 (*SP*) (JNK inhibitor, 10 μM), KN-93 (*KN*) $Ca^{2+}$/calmodulin-dependent kinase II (*CaMKII*, 10 μM), cyclosporin A (*CsA*) (10 μM), bisindolylmaleimide I (*BIM-I*) (PKC inhibitor, 2.5 μM), and Gö-6976 (*Gö*) ( specific inhibitor of calcium-responsive PKCs, 10 μM) for 6 h and then lysed for luciferase activity determination. Data are expressed as mean ± S.E. from at least three different determinations ***, $p < 0.001$.

Both $IP_3R$ blockade with XeC ($IP_3R$ blocker) and U-73122 (PLC inhibitor) treatment resulted in 25 and 22% reduction in the $[Ca^{2+}]_{rest}$ in *mdx* myotubes, respectively. These combined data strongly demonstrate that the SR plays an important role in the dysregulation $[Ca^{2+}]_{rest}$ observed in dystrophic myotubes.

There is a controversy concerning the SR $Ca^{2+}$ levels in *mdx* skeletal muscle cells. Robert *et al.* (57) demonstrated an increased SR $Ca^{2+}$ loading capacity after depletion in *mdx* compared with WT. However, other authors have shown a reduced expression of calsequestrin-like proteins, lower SR $Ca^{2+}$ loading (58), and reduced sarco/endoplasmic reticulum $Ca^{2+}$-ATPase activity in *mdx* muscles (59). Recently, Robin *et al.* (60) demonstrated an elevated passive SR $Ca^{2+}$ leak in *mdx* fibers, using fibers voltage-clamped at −80 mV and exposed to cyclopiazonic acid. Our results have shown that Ry- or XeC-treated *mdx* myotubes have an increase in SR $Ca^{2+}$ store content suggesting that SR leak occurs through these $Ca^{2+}$ channels. SERCA1a overexpression in *mdx* diaphragm muscle by adeno-associated virus gene transfer resulted in a reduction of centrally located nuclei and reduced susceptibility to eccentric contraction-induced damage (61). More recently, δ-sarcoglycan-null and *mdx* mice animals that overexpress SERCA1 through transgenesis show an improvement in muscle damage and excitation-contraction coupling and restore the $[Ca^{2+}]_{rest}$ and $[Ca^{2+}]_{SR}$ in both dystrophic models (62). Together, this suggests that the filling state of the SR contributes significantly to the dysregulation $[Ca^{2+}]_{rest}$ observed in *mdx* muscles.

Several reports indicate that resting membrane potentials are more positive in *mdx* muscles fibers than WT (27, 63–65). We have found that *mdx* myotubes showed a partial membrane depolarization compared with WT. None of the drugs used in this study, all of which have a major effect on $[Ca^{2+}]_{rest}$, induced a significant repolarization in the *mdx* myotubes. These are not surprising results because none of them have any effect on ion permeability or ion-translocat-

ing enzymes involved in maintaining the resting membrane potential value.

Numerous facts indicate that the dystrophic skeletal muscle cells have impaired excitation-contraction coupling. Comparisons of the cytosolic $Ca^{2+}$ transients evoked by a single action potential have shown that the $Ca^{2+}$ transients are reduced in *mdx* and *mdx*;*utr*$^{-/-}$ fibers compared with WT fibers (66–68). Muscle weakness observed in isolated fibers from *mdx* mice and DMD patients has not been fully explained. The reduction in the $Ca^{2+}$ transient evoked by single action potential, increased $V_m$, increased $[Ca^{2+}]_{rest}$, and a reduced $Ca^{2+}$ loading capacity of the SR could provide a mechanism for contractile dysfunction and impaired force production in DMD patients.

Several studies have shown that NF-κB activity is increased in *mdx* skeletal muscles (8–15), but the mechanisms causing this abnormality have not been previously unveiled. Acharyya *et al.* (10) reported an increased NF-κB DNA binding activity and IKK activation, without any change in IκBα expression and phosphorylation and normal levels of p65 with an increased phosphorylation. The authors proposed direct p65 activation by IKKβ (10). On the contrary, Singh *et al.* (15) have found an increase in the expression of both p65 and IκBα and increased IκBα phosphorylation, indicating that NF-κB activation in *mdx* muscles is due to a complex mechanism and not only IKK activation. Both examined activation of NF-κB in whole muscle extracts. Because dystrophic muscles are associated with a large amount of activated immune cell infiltrates, which have increased NF-κB activity (7, 10), it is possible that this increase was not due to changes in muscle cells. Here, we used the myotube model to determine whether NF-κB can be activated in dystrophic skeletal muscle cells without contribution from the immune system. We observed that NF-κB transcriptional activity, measured by a luciferase reporter, was increased in *mdx* myotubes, and we observed a significant increase in p65 nucleus/cytosol fluorescence. Both luciferase activity and p65 nuclear localization could be reduced by agents that modulate $[Ca^{2+}]_{rest}$ in *mdx* myotubes but were not changed by these drugs in WT myotubes.

We do not know the exact mechanism that accounts for $[Ca^{2+}]_{rest}$-dependent activation of NF-κB in muscle cells. Several $Ca^{2+}$-sensitive pathways can modulate the activity of NF-κB (41). We have previously shown that membrane depolarization activates NF-κB through increases in intracellular $Ca^{2+}$ through RyR and $IP_3R$. This $Ca^{2+}$-dependent modulation has been attributed to calcineurin A, PKC, and ERK1/2 pathway activation in normal myotubes (40). We have not found any significant effect in the luciferase activity when we preincubated with specific blockers of these signaling pathways in WT and *mdx* myotubes. Similar results were obtained with $Ca^{2+}$/calmodulin-dependent kinase II and JNK inhibitors. Surprisingly, p38 inhibition by SB-203580 dramatically reduced the luciferase activity of the NF-κB reporter. The p38 MAPK is activated by various stimuli, including exercise, contraction, insulin, environmental stress, and pro-inflammatory cytokines (69). SB-203580 is a specific blocker of the p38 MAPK that inhibits the catalytic activity of this protein (70).

Badger *et al.* (71) has shown that SB-203580 blocks IL-1-induced p38 kinase activity, NO production, and iNOS expression in chondrocytes. In addition, in C6 glioma cells, the stimulation with LPS increases iNOS mRNA expression, NO production, phosphorylation of p38, and the activation of NF-κB. Treatment with SB-203580 reduced iNOS expression and NO production; however, it did not modify the NF-κB DNA binding activity (72).

Nakamura *et al.* (73) have shown that calcineurin A, JNK1, and p38 signaling pathways were constantly activated in dystrophic *mdx*;*utr*$^{-/-}$ hearts, associated with an increased p38 phosphorylation. However, in skeletal muscle, a reduction in p38 phosphorylation has been shown but was accompanied by an increase in p38 protein expression in whole lysates from *mdx* tibialis anterior muscles (74). Several reports have shown that calcium activates p38 MAPK, but the mechanisms by which it does so are poorly understood. In cerebellar granular cells, glutamate stimulates the activity of p38 through $Ca^{2+}$ entry from extracellular space and Rho GTPase activation (75, 76). In myotubes, caffeine increases p38 phosphorylation via $Ca^{2+}$/calmodulin-dependent kinase II activation and participates in the expression of PGC-1α and mitochondrial biogenesis (77). Further studies will be required to clarify this issue in *mdx* skeletal muscle cells and the precise mechanism involved in the NF-κB activation.

Finally, we observed that iNOS expression could also be modulated by $[Ca^{2+}]_{rest}$ through NF-κB under resting conditions. p65 knockdown normalized the iNOS protein levels in *mdx* myotubes to WT levels, similar to the effect of the agents that lowered $[Ca^{2+}]_{rest}$ had on iNOS mRNA expression; iNOS overexpression by this mechanism could be responsible for the oxidative and nitrosative stress observed in *mdx* muscles (26) and can provide a positive loop for $Ca^{2+}$ deregulation in dystrophic skeletal muscle cells.

Overexpression of TRPC3 (skeletal muscle-specific transgenic mice) and the associated increase in calcium influx resulted in a phenotype of muscular dystrophy (78). The authors have shown an increase in central nucleation of fibers, increased numbers of smaller myofibers, fibrosis, and infiltration of inflammatory cells. Moreover, sarco/endoplasmic reticulum $Ca^{2+}$-ATPase overexpression in *Sgcg*$^{-/-}$, *mdx,* and in TRPC3 transgenic mice mitigated biochemical and histological features of muscular dystrophy improving the altered intracellular $Ca^{2+}$ handling (62). As described above, *S*-nitrosylation of RyR induces $Ca^{2+}$ alterations related with an augmented spontaneous $Ca^{2+}$ spark frequency (22). In addition, transient receptor potential channels elicited robust elevation of $Ca^{2+}$ in response to the NO donor *S*-nitroso-*N*-acetyl-DL-penicillamine, especially TRPC5 (79). TRPC5, TRPA1, and TRPM1 channels were increased in *mdx* skeletal muscle at certain stages (80). These modifications induced by NO could exacerbate the pathology in *mdx* muscles.

We did not find any difference in cytokine expression in *mdx* myotubes (supplemental Fig. S3). Because macrophages and lymphocytes are specialized immune cells (infiltrated in dystrophic muscle), we think that they may be responsible for the secretion of these cytokines. This hypothesis is reinforced by IKKβ (upstream activator of NF-κB) deletion in myeloid cells from *mdx* mice, a procedure that reduced inflammation and concomitantly TNF-α and IL-1β expression (10). In addition,

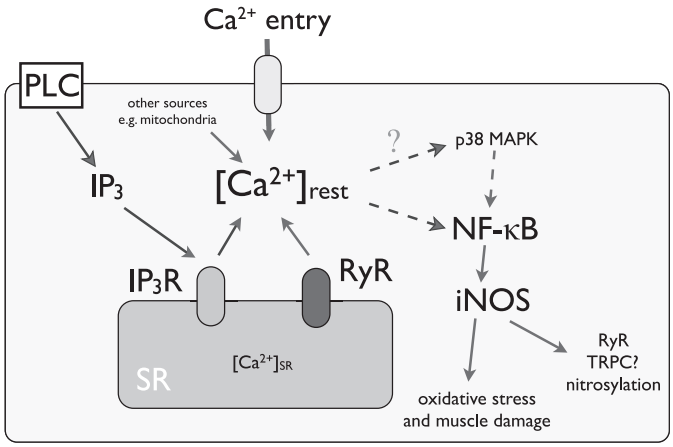


FIGURE 7. **Proposed model for $[Ca^{2+}]_{rest}$ deregulation, NF-κB up-regulation, and iNOS expression in *mdx* myotubes.** In addition to the $Ca^{2+}$ entry through reported TRPC1 and SOCE ($Gd^{3+}$ sensitive), $[Ca^{2+}]_{rest}$ deregulation in *mdx* myotubes is a complex event that involves $Ca^{2+}$ entry and SR $Ca^{2+}$ leak through RyR ad $IP_3R$. The data collected in this work suggest that increased $[Ca^{2+}]_{rest}$, increases NF-κB and iNOS expression in dystrophic myotubes. *PLC*, phospholipase C.

production of pro-inflammatory cytokines is probably a complex process that requires simultaneous activation of pathways other than NF-κB. iNOS promoter has two *bona fide* NF-κB-binding sites (reviewed in Ref. 81). TNF-α is often described as one of the classical NF-κB-dependent cytokines. However, there are numerous contradictory data for a role for NF-κB as a classic activator of TNF-α, and it seems that expression of this cytokine requires nuclear factor of activated T-cells activation, as well as other co-activators (reviewed in Ref. 82).

In summary, we have found that increased $[Ca^{2+}]_{rest}$ is modulated by $Ca^{2+}$ entry as a result of SR unloading caused by $Ca^{2+}$ leak through RyR and $IP_3R$ in dystrophic myotubes and that this alteration increases NF-κB activity and iNOS expression, likely through p38 activation. These mechanisms can provide several potential therapy targets to improve muscle degeneration observed in DMD patients and explain the progressive damage observed in this pathology (Fig. 7).

*Acknowledgments—We thank Dr. Claudio F. Perez and Dr. Karen Westerman for their help in designing our experimental procedures. We also acknowledge Dr. Peter Schupp for the gift of Ianthella basta.*

## REFERENCES


1. Blake, D. J., Weir, A., Newey, S. E., and Davies, K. E. (2002) Function and genetics of dystrophin and dystrophin-related proteins in muscle. *Physiol. Rev.* **82,** 291–329
2. Emery, A. E. (2002) The muscular dystrophies. *Lancet* **359,** 687–695
3. Henry, M. D., and Campbell, K. P. (1996) Dystroglycan. An extracellular matrix receptor linked to the cytoskeleton. *Curr. Opin. Cell Biol.* **8,** 625–631
4. Pasternak, C., Wong, S., and Elson, E. L. (1995) Mechanical function of dystrophin in muscle cells. *J. Cell Biol.* **128,** 355–361
5. Petrof, B. J., Shrager, J. B., Stedman, H. H., Kelly, A. M., and Sweeney, H. L. (1993) Dystrophin protects the sarcolemma from stresses developed during muscle contraction. *Proc. Natl. Acad. Sci. U.S.A.* **90,** 3710–3714
6. Evans, N. P., Misyak, S. A., Robertson, J. L., Bassaganya-Riera, J., and Grange, R. W. (2009) Immune-mediated mechanisms potentially regulate the disease time course of Duchenne muscular dystrophy and provide targets for therapeutic intervention. *PM R* **1,** 755–768
7. Oeckinghaus, A., and Ghosh, S. (2009) The NF-κB family of transcription factors and its regulation. *Cold Spring Harbor Perspect. Biol.* **1,** a000034
8. Siegel, A. L., Bledsoe, C., Lavin, J., Gatti, F., Berge, J., Millman, G., Turin, E., Winders, W. T., Rutter, J., Palmeiri, B., and Carlson, C. G. (2009) Treatment with inhibitors of the NF-κB pathway improves whole body tension development in the mdx mouse. *Neuromuscul. Disord.* **19,** 131–139
9. Pan, Y., Chen, C., Shen, Y., Zhu, C. H., Wang, G., Wang, X. C., Chen, H. Q., and Zhu, M. S. (2008) Curcumin alleviates dystrophic muscle pathology in mdx mice. *Mol. Cells* **25,** 531–537
10. Acharyya, S., Villalta, S. A., Bakkar, N., Bupha-Intr, T., Janssen, P. M., Carathers, M., Li, Z. W., Beg, A. A., Ghosh, S., Sahenk, Z., Weinstein, M., Gardner, K. L., Rafael-Fortney, J. A., Karin, M., Tidball, J. G., Baldwin, A. S., and Guttridge, D. C. (2007) Interplay of IKK/NF-κB signaling in macrophages and myofibers promotes muscle degeneration in Duchenne muscular dystrophy. *J. Clin. Invest.* **117,** 889–901
11. Tang, Y., Reay, D. P., Salay, M. N., Mi, M. Y., Clemens, P. R., Guttridge, D. C., Robbins, P. D., Huard, J., and Wang, B. (2010) Inhibition of the IKK/NF-κB pathway by AAV gene transfer improves muscle regeneration in older mdx mice. *Gene Ther.* **17,** 1476–1483
12. Messina, S., Bitto, A., Aguennouz, M., Minutoli, L., Monici, M. C., Altavilla, D., Squadrito, F., and Vita, G. (2006) Nuclear factor-κB blockade reduces skeletal muscle degeneration and enhances muscle function in Mdx mice. *Exp. Neurol.* **198,** 234–241
13. Dogra, C., Srivastava, D. S., and Kumar, A. (2008) Protein-DNA array-based identification of transcription factor activities differentially regulated in skeletal muscle of normal and dystrophin-deficient mdx mice. *Mol. Cell. Biochem.* **312,** 17–24
14. Durham, W. J., Arbogast, S., Gerken, E., Li, Y. P., and Reid, M. B. (2006) Progressive nuclear factor-κB activation resistant to inhibition by contraction and curcumin in mdx mice. *Muscle Nerve* **34,** 298–303
15. Singh, R., Millman, G., Turin, E., Polisiakeiwicz, L., Lee, B., Gatti, F., Berge, J., Smith, E., Rutter, J., Sumski, C., Winders, W. T., Samadi, A., and Carlson, C. G. (2009) Increases in nuclear p65 activation in dystrophic skeletal muscle are secondary to increases in the cellular expression of p65 and are not solely produced by increases in IκB-α kinase activity. *J. Neurol. Sci.* **285,** 159–171
16. Tak, P. P., and Firestein, G. S. (2001) NF-κB. A key role in inflammatory diseases. *J. Clin. Invest.* **107,** 7–11
17. Hnia, K., Gayraud, J., Hugon, G., Ramonatxo, M., De La Porte, S., Matecki, S., and Mornet, D. (2008) L-Arginine decreases inflammation and modulates the nuclear factor-κB/matrix metalloproteinase cascade in mdx muscle fibers. *Am. J. Pathol.* **172,** 1509–1519
18. Kumar, A., and Boriek, A. M. (2003) Mechanical stress activates the nuclear factor-κB pathway in skeletal muscle fibers. A possible role in Duchenne muscular dystrophy. *FASEB J.* **17,** 386–396
19. Porreca, E., Guglielmi, M. D., Uncini, A., Di Gregorio, P., Angelini, A., Di Febbo, C., Pierdomenico, S. D., Baccante, G., and Cuccurullo, F. (1999) Hemostatic abnormalities, cardiac involvement, and serum tumor necrosis factor levels in X-linked dystrophic patients. *Thromb. Haemost.* **81,** 543–546
20. Porter, J. D., Khanna, S., Kaminski, H. J., Rao, J. S., Merriam, A. P., Richmonds, C. R., Leahy, P., Li, J., Guo, W., and Andrade, F. H. (2002) A chronic inflammatory response dominates the skeletal muscle molecular signature in dystrophin-deficient mdx mice. *Hum. Mol. Genet.* **11,** 263–272
21. Ji, L. L. (2008) Modulation of skeletal muscle antioxidant defense by exercise. Role of redox signaling. *Free Radic. Biol. Med.* **44,** 142–152
22. Bellinger, A. M., Reiken, S., Carlson, C., Mongillo, M., Liu, X., Rothman, L., Matecki, S., Lacampagne, A., and Marks, A. R. (2009) Hypernitrosylated ryanodine receptor calcium release channels are leaky in dystrophic muscle. *Nat. Med.* **15,** 325–330
23. Louboutin, J. P., Rouger, K., Tinsley, J. M., Halldorson, J., and Wilson, J. M. (2001) iNOS expression in dystrophinopathies can be reduced by somatic gene transfer of dystrophin or utrophin. *Mol. Med.* **7,** 355–364
24. Pacher, P., Beckman, J. S., and Liaudet, L. (2007) Nitric oxide and peroxynitrite in health and disease. *Physiol. Rev.* **87,** 315–424
25. Yeung, E. W., Whitehead, N. P., Suchyna, T. M., Gottlieb, P. A., Sachs, F., and Allen, D. G. (2005) Effects of stretch-activated channel blockers on

$[Ca^{2+}]_i$ and muscle damage in the mdx mouse. *J. Physiol.* **562,** 367–380
26. Whitehead, N. P., Yeung, E. W., and Allen, D. G. (2006) Muscle damage in mdx (dystrophic) mice. Role of calcium and reactive oxygen species. *Clin. Exp. Pharmacol. Physiol.* **33,** 657–662
27. López, J. R., Briceño, L. E., Sánchez, V., and Horvart, D. (1987) Myoplasmic $[Ca^{2+}]$ in Duchenne muscular dystrophy patients. *Acta Cient. Venez.* **38,** 503–504
28. Allen, D. G., Gervasio, O. L., Yeung, E. W., and Whitehead, N. P. (2010) Calcium and the damage pathways in muscular dystrophy. *Can. J. Physiol. Pharmacol.* **88,** 83–91
29. Turner, P. R., Westwood, T., Regen, C. M., and Steinhardt, R. A. (1988) Increased protein degradation results from elevated free calcium levels found in muscle from mdx mice. *Nature* **335,** 735–738
30. Bakker, A. J., Head, S. I., Williams, D. A., and Stephenson, D. G. (1993) $Ca^{2+}$ levels in myotubes grown from the skeletal muscle of dystrophic (mdx) and normal mice. *J. Physiol.* **460,** 1–13
31. Gailly, P., Boland, B., Himpens, B., Casteels, R., and Gillis, J. M. (1993) Critical evaluation of cytosolic calcium determination in resting muscle fibers from normal and dystrophic (mdx) mice. *Cell Calcium* **14,** 473–483
32. Pressmar, J., Brinkmeier, H., Seewald, M. J., Naumann, T., and Rüdel, R. (1994) Intracellular $Ca^{2+}$ concentrations are not elevated in resting cultured muscle from Duchenne (DMD) patients and in MDX mouse muscle fibers. *Pflugers Arch.* **426,** 499–505
33. Mokri, B., and Engel, A. G. (1998) Duchenne dystrophy. Electron microscopic findings point to a basic or early abnormality in the plasma membrane of the muscle fiber. *Neurology* **51,** 1–10
34. Vandebrouck, C., Martin, D., Colson-Van Schoor, M., Debaix, H., and Gailly, P. (2002) Involvement of TRPC in the abnormal calcium influx observed in dystrophic (mdx) mouse skeletal muscle fibers. *J. Cell Biol.* **158,** 1089–1096
35. Vandebrouck, A., Ducret, T., Basset, O., Sebille, S., Raymond, G., Ruegg, U., Gailly, P., Cognard, C., and Constantin, B. (2006) Regulation of store-operated calcium entries and mitochondrial uptake by minidystrophin expression in cultured myotubes. *FASEB J.* **20,** 136–138
36. Gervásio, O. L., Whitehead, N. P., Yeung, E. W., Phillips, W. D., and Allen, D. G. (2008) TRPC1 binds to caveolin-3 and is regulated by Src kinase. Role in Duchenne muscular dystrophy. *J. Cell Sci.* **121,** 2246–2255
37. Edwards, J. N., Friedrich, O., Cully, T. R., von Wegner, F., Murphy, R. M., and Launikonis, B. S. (2010) Up-regulation of store-operated $Ca^{2+}$ entry in dystrophic mdx mouse muscle. *Am. J. Physiol. Cell Physiol* **299,** C42–C50
38. Boittin, F. X., Petermann, O., Hirn, C., Mittaud, P., Dorchies, O. M., Roulet, E., and Ruegg, U. T. (2006) $Ca^{2+}$-independent phospholipase $A_2$ enhances store-operated $Ca^{2+}$ entry in dystrophic skeletal muscle fibers. *J. Cell Sci.* **119,** 3733–3742
39. Riquelme, D., Alvarez, A., Leal, N., Adasme, T., Espinoza, I., Valdés, J. A., Troncoso, N., Hartel, S., Hidalgo, J., Hidalgo, C., and Carrasco, M. A. (2011) High frequency field stimulation of primary neurons enhances ryanodine receptor-mediated $Ca^{2+}$ release and generates hydrogen peroxide, which jointly stimulate NF-κB activity. *Antioxid. Redox. Signal.* **14,** 1245–1259
40. Valdés, J. A., Hidalgo, J., Galaz, J. L., Puentes, N., Silva, M., Jaimovich, E., and Carrasco, M. A. (2007) NF-κB activation by depolarization of skeletal muscle cells depends on ryanodine and $IP_3$ receptor-mediated calcium signals. *Am. J. Physiol. Cell Physiol.* **292,** C1960–C1970
41. Lilienbaum, A., and Israël, A. (2003) From calcium to NF-κB signaling pathways in neurons. *Mol. Cell. Biol.* **23,** 2680–2698
42. Sée, V., Rajala, N. K., Spiller, D. G., and White, M. R. (2004) Calcium-dependent regulation of the cell cycle via a novel MAPK-NF-κB pathway in Swiss 3T3 cells. *J. Cell Biol.* **166,** 661–672
43. Spencer, M. J., Croall, D. E., and Tidball, J. G. (1995) Calpains are activated in necrotic fibers from *mdx* dystrophic mice. *J. Biol. Chem.* **270,** 10909–10914
44. Millay, D. P., Sargent, M. A., Osinska, H., Baines, C. P., Barton, E. R., Vuagniaux, G., Sweeney, H. L., Robbins, J., and Molkentin, J. D. (2008) Genetic and pharmacologic inhibition of mitochondria dependent necrosis attenuates muscular dystrophy. *Nat. Med.* **14,** 442–447
45. Rando, T. A., and Blau, H. M. (1994) Primary mouse myoblast purification, characterization, and transplantation for cell-mediated gene therapy. *J. Cell Biol.* **125,** 1275–1287
46. Casas, M., Altamirano, F., and Jaimovich, E. (2012) Measurement of calcium release due to inositol trisphosphate receptors in skeletal muscle. *Methods Mol. Biol.* **798,** 383–393
47. Eltit, J. M., Yang, T., Li, H., Molinski, T. F., Pessah, I. N., Allen, P. D., and Lopez, J. R. (2010) RyR1-mediated $Ca^{2+}$ leak and $Ca^{2+}$ entry determine resting intracellular $Ca^{2+}$ in skeletal myotubes. *J. Biol. Chem.* **285,** 13781–13787
48. Westerman, K. A., Penvose, A., Yang, Z., Allen, P. D., and Vacanti, C. A. (2010) Adult muscle "stem" cells can be sustained in culture as free-floating myospheres. *Exp. Cell Res.* **316,** 1966–1976
49. Livak, K. J., and Schmittgen, T. D. (2001) Analysis of relative gene expression data using real time quantitative PCR and the $2(-\Delta\Delta C_T)$ method. *Methods* **25,** 402–408
50. Marshall, O. J. (2004) PerlPrimer. Cross-platform, graphical primer design for standard, bisulfite, and real time PCR. *Bioinformatics* **20,** 2471–2472
51. Mack, M. M., Molinski, T. F., Buck, E. D., and Pessah, I. N. (1994) Novel modulators of skeletal muscle FKBP12/calcium channel complex from *Ianthella basta.* Role of FKBP12 in channel gating. *J. Biol. Chem.* **269,** 23236–23249
52. Liberona, J. L., Powell, J. A., Shenoi, S., Petherbridge, L., Caviedes, R., and Jaimovich, E. (1998) Differences in both inositol 1,4,5-trisphosphate mass and inositol 1,4,5-trisphosphate receptors between normal and dystrophic skeletal muscle cell lines. *Muscle Nerve* **21,** 902–909
53. Casas, M., Figueroa, R., Jorquera, G., Escobar, M., Molgó, J., and Jaimovich, E. (2010) $IP_3$-dependent post-tetanic calcium transients induced by electrostimulation of adult skeletal muscle fibers. *J. Gen. Physiol.* **136,** 455–467
54. Jaimovich, E., Mattei, C., Liberona, J. L., Cardenas, C., Estrada, M., Barbier, J., Debitus, C., Laurent, D., and Molgó, J. (2005) Xestospongin B, a competitive inhibitor of $IP_3$-mediated $Ca^{2+}$ signaling in cultured rat myotubes, isolated myonuclei, and neuroblastoma (NG108-15) cells. *FEBS Lett.* **579,** 2051–2057
55. Ho, R. C., Hirshman, M. F., Li, Y., Cai, D., Farmer, J. R., Aschenbach, W. G., Witczak, C. A., Shoelson, S. E., and Goodyear, L. J. (2005) Regulation of Iκ B kinase and NF-κB in contracting adult rat skeletal muscle. *Am. J. Physiol. Cell Physiol.* **289,** C794–C801
56. Várnai, P., Hunyady, L., and Balla, T. (2009) STIM and Orai. The long-awaited constituents of store-operated calcium entry. *Trends Pharmacol. Sci.* **30,** 118–128
57. Robert, V., Massimino, M. L., Tosello, V., Marsault, R., Cantini, M., Sorrentino, V., and Pozzan, T. (2001) Alteration in calcium handling at the subcellular level in *mdx* myotubes. *J. Biol. Chem.* **276,** 4647–4651
58. Culligan, K., Banville, N., Dowling, P., and Ohlendieck, K. (2002) Drastic reduction of calsequestrin-like proteins and impaired calcium binding in dystrophic mdx muscle. *J. Appl. Physiol.* **92,** 435–445
59. Kargacin, M. E., and Kargacin, G. J. (1996) The sarcoplasmic reticulum calcium pump is functionally altered in dystrophic muscle. *Biochim. Biophys. Acta* **1290,** 4–8
60. Robin, G., Berthier, C., and Allard, B. (2012) Sarcoplasmic reticulum $Ca^{2+}$ permeation explored from the lumen side in mdx muscle fibers under voltage control. *J. Gen. Physiol.* **139,** 209–218
61. Morine, K. J., Sleeper, M. M., Barton, E. R., and Sweeney, H. L. (2010) Overexpression of SERCA1a in the mdx diaphragm reduces susceptibility to contraction-induced damage. *Hum. Gene Ther.* **21,** 1735–1739
62. Goonasekera, S. A., Lam, C. K., Millay, D. P., Sargent, M. A., Hajjar, R. J., Kranias, E. G., and Molkentin, J. D. (2011) Mitigation of muscular dystrophy in mice by SERCA overexpression in skeletal muscle. *J. Clin. Invest.* **121,** 1044–1052
63. Carlson, C. G., Samadi, A., and Siegel, A. (2005) Chronic treatment with agents that stabilize cytosolic Iκ B-α enhances survival and improves resting membrane potential in MDX muscle fibers subjected to chronic passive stretch. *Neurobiol. Dis.* **20,** 719–730
64. Miles, M. T., Cottey, E., Cottey, A., Stefanski, C., and Carlson, C. G. (2011) Reduced resting potentials in dystrophic (mdx) muscle fibers are secondary to NF-κB-dependent negative modulation of ouabain-sensitive $Na^+$-$K^+$ pump activity. *J. Neurol. Sci.* **303,** 53–60

65. Carlson, C. G., and Roshek, D. M. (2001) Adult dystrophic (mdx) end plates exhibit reduced quantal size and enhanced quantal variation. *Pflugers Arch.* **442,** 369–375
66. Woods, C. E., Novo, D., DiFranco, M., and Vergara, J. L. (2004) The action potential evoked sarcoplasmic reticulum calcium release is impaired in mdx mouse muscle fibers. *J. Physiol.* **557,** 59–75
67. Hollingworth, S., Zeiger, U., and Baylor, S. M. (2008) Comparison of the myoplasmic calcium transient elicited by an action potential in intact fibers of mdx and normal mice. *J. Physiol.* **586,** 5063–5075
68. Capote, J., DiFranco, M., and Vergara, J. L. (2010) Excitation-contraction coupling alterations in mdx and utrophin/dystrophin double knockout mice. A comparative study. *Am. J. Physiol. Cell Physiol.* **298,** C1077–C1086
69. Röckl, K. S., Witczak, C. A., and Goodyear, L. J. (2008) Signaling mechanisms in skeletal muscle. Acute responses and chronic adaptations to exercise. *IUBMB Life* **60,** 145–153
70. Kumar, S., Jiang, M. S., Adams, J. L., and Lee, J. C. (1999) Pyridinylimidazole compound SB-203580 inhibits the activity but not the activation of p38 mitogen-activated protein kinase. *Biochem. Biophys. Res. Commun.* **263,** 825–831
71. Badger, A. M., Cook, M. N., Lark, M. W., Newman-Tarr, T. M., Swift, B. A., Nelson, A. H., Barone, F. C., and Kumar, S. (1998) SB-203580 inhibits p38 mitogen-activated protein kinase, nitric oxide production, and inducible nitric oxide synthase in bovine cartilage-derived chondrocytes. *J. Immunol.* **161,** 467–473
72. Won, J. S., Lee, J. K., and Suh, H. W. (2001) Forskolin inhibits expression of inducible nitric-oxide synthase mRNA via inhibiting the mitogen-activated protein kinase in C6 cells. *Brain Res. Mol. Brain Res.* **89,** 1–10
73. Nakamura, A., Harrod, G. V., and Davies, K. E. (2001) Activation of calcineurin and stress-activated protein kinase/p38-mitogen-activated protein kinase in hearts of utrophin-dystrophin knockout mice. *Neuromuscul. Disord.* **11,** 251–259
74. Ljubicic, V., Khogali, S., Renaud, J. M., and Jasmin, B. J. (2012) Chronic AMPK stimulation attenuates adaptive signaling in dystrophic skeletal muscle. *Am. J. Physiol. Cell Physiol.* **302,** C110–C121
75. Kawasaki, H., Morooka, T., Shimohama, S., Kimura, J., Hirano, T., Gotoh, Y., and Nishida, E. (1997) Activation and involvement of p38 mitogen-activated protein kinase in glutamate-induced apoptosis in rat cerebellar granule cells. *J. Biol. Chem.* **272,** 18518–18521
76. Semenova, M. M., Mäki-Hokkonen, A. M., Cao, J., Komarovski, V., Forsberg, K. M., Koistinaho, M., Coffey, E. T., and Courtney, M. J. (2007) Rho mediates calcium-dependent activation of p38α and subsequent excitotoxic cell death. *Nat. Neurosci.* **10,** 436–443
77. Wright, D. C., Geiger, P. C., Han, D. H., Jones, T. E., and Holloszy, J. O. (2007) Calcium induces increases in peroxisome proliferator-activated receptor γ coactivator-1α and mitochondrial biogenesis by a pathway leading to p38 mitogen-activated protein kinase activation. *J. Biol. Chem.* **282,** 18793–18799
78. Millay, D. P., Goonasekera, S. A., Sargent, M. A., Maillet, M., Aronow, B. J., and Molkentin, J. D. (2009) Calcium influx is sufficient to induce muscular dystrophy through a TRPC-dependent mechanism. *Proc. Natl. Acad. Sci. U.S.A.* **106,** 19023–19028
79. Yoshida, T., Inoue, R., Morii, T., Takahashi, N., Yamamoto, S., Hara, Y., Tominaga, M., Shimizu, S., Sato, Y., and Mori, Y. (2006) Nitric oxide activates TRP channels by cysteine *S*-nitrosylation. *Nat. Chem. Biol.* **2,** 596–607
80. Krüger, J., Kunert-Keil, C., Bisping, F., and Brinkmeier, H. (2008) Transient receptor potential cation channels in normal and dystrophic mdx muscle. *Neuromuscul. Disord.* **18,** 501–513
81. Kleinert, H., Schwarz, P. M., and Förstermann, U. (2003) Regulation of the expression of inducible nitric-oxide synthase. *Biol. Chem.* **384,** 1343–1364
82. Falvo, J. V., Tsytsykova, A. V., and Goldfeld, A. E. (2010) Transcriptional control of the TNF gene. *Curr. Dir. Autoimmun.* **11,** 27–60
83. Buvinic, S., Almarza, G., Bustamante, M., Casas, M., López, J., Riquelme, M., Sáez, J. C., Huidobro-Toro, J. P., and Jaimovich, E. (2009) ATP released by electrical stimuli elicits calcium transients and gene expression in skeletal muscle. *J. Biol. Chem.* **284,** 34490–34505